

1 **Consistency evaluation of tropospheric ozone from ozonesonde and**  
2 **IAGOS aircraft observations: vertical distribution, ozonesonde types**  
3 **and station-airport distance**

4 Honglei Wang<sup>1, 2</sup>, David W. Tarasick<sup>3\*</sup>, Jane Liu<sup>2\*</sup>, Herman G.J. Smit<sup>4</sup>, Roeland Van Malderen<sup>5</sup>,  
5 Lijuan Shen<sup>6</sup>, Romain Blot<sup>7</sup>, Tianliang Zhao<sup>1</sup>

6 <sup>1</sup> China Meteorological Administration Aerosol-Cloud and Precipitation Key Laboratory, Nanjing University of  
7 Information Science and Technology, Nanjing, 210044, China

8 <sup>2</sup> Department of Geography and Planning, University of Toronto, Toronto, M5S 3G3, Canada

9 <sup>3</sup> Environment and Climate Change Canada, 4905 Dufferin Street, Downsview, M3H 5T4, Canada

10 <sup>4</sup> Institute for Energy and Climate Research: Troposphere (IEK-8), Research Centre Juelich (FZJ), Juelich, Germany

11 <sup>5</sup> Royal Meteorological Institute of Belgium, Brussels, Belgium

12 <sup>6</sup> School of Atmosphere and Remote Sensing, Wuxi University, Wuxi, 214105, China

13 <sup>7</sup> Laboratoire d'Aérodologie (LAERO), Université de Toulouse, CNRS, Toulouse, France

14 \* Corresponding authors: David.Tarasick@ec.gc.ca and janejj.liu@utoronto.ca

15

16 **Abstract:** The vertical distribution of tropospheric O<sub>3</sub> from ozonesondes is compared with that from  
17 In-service Aircraft for a Global Observing System (IAGOS) measurements at 23 pairs of sites  
18 between about 30°S and 55°N, from 1995 to 2021. Profiles of tropospheric O<sub>3</sub> from IAGOS aircraft  
19 are in generally good agreement with ozonesonde observations, for Electrochemical concentration  
20 cells (ECC), Brewer-Mast, and Carbon-Iodine sensors, with average biases of 2.58 ppb, -0.28 ppb,  
21 and 0.67 ppb, and correlation coefficients (R) of 0.72, 0.82, and 0.66, respectively. Agreement  
22 between the aircraft and Indian-sonde observations is poor, with an average bias of 15.32 ppb and  
23 R of 0.44. The O<sub>3</sub> concentration observed by ECC sondes is on average higher by 5-10% than that  
24 observed by IAGOS aircraft, and the relative bias increases modestly with altitude. For other sonde  
25 types, there are some seasonal and altitude variations in the relative bias with respect to IAGOS  
26 measurements, but these appear to be caused by local differences. The distance between station and  
27 airport within 4° has little effect on the comparison results. For the ECC ozonesonde, the overall  
28 bias with respect to IAGOS measurements varies from 5.7 to 9.8 ppb, when the station pairs are  
29 grouped by station-airport distances of <1° (latitude and longitude), 1-2°, and 2-4°. Correlations for

30 these groups are  $R = 0.8, 0.9$  and  $0.7$ . These comparison results provide important information for  
31 merging ozonesonde and IAGOS measurement datasets. They can also be used to evaluate the  
32 relative biases of the different sonde types in the troposphere, using the aircraft as a transfer standard.

33 **Key words:** WOUDC; IAGOS; tropospheric  $O_3$ ; vertical distribution; ozonesonde; aircraft

34

## 35 **1 Introduction**

36 Ozone ( $O_3$ ) is a trace gas with small concentrations in the atmosphere (Ramanathan et al., 1985). It  
37 is an important greenhouse gas in the upper troposphere. In the planetary boundary layer, it is a  
38 major air pollutant (Lefohn et al., 2018; Monks et al., 2015). It can endanger human health, damage  
39 ecosystems, and affect climate change (Fu and Tai, 2015; Lefohn et al., 2018; Percy et al., 2003).  
40 Therefore, it is of importance to study the temporal and spatial variations in tropospheric  $O_3$   
41 including near-surface  $O_3$  and mechanisms affecting the variations (Logan, 1985; Ma et al., 2020;  
42 Sharma et al., 2017; Young et al., 2018).

43 A large number of studies have been carried out on the spatiotemporal distribution, formation  
44 mechanisms, and transport characteristics of tropospheric  $O_3$  (Li et al., 2020, 2021; Vingarzan, 2004;  
45 Wang et al., 2017, 2023; Xu et al., 2021; Yu et al., 2021). However, due to the limitation of  
46 observations, there are many unknowns on tropospheric  $O_3$ , especially the vertical distribution of  
47 tropospheric  $O_3$ . Satellites provide an effective platform for measuring  $O_3$  globally. Satellite  $O_3$   
48 instruments, including TES, GOME, GOME-2, SCIAMACHY, OMI, and TROPOMI, have been in  
49 operation for decades (David et al., 2013; Ebojie et al., 2016; Hegarty et al., 2009; Hoogen et al.,  
50 1999; Hubert et al., 2021; Miles et al., 2015). Although satellite observations can provide detailed  
51 temporally- and horizontally-resolved maps of tropospheric  $O_3$  columns, in general satellite data  
52 lack vertical resolution. While tropospheric differential absorption lidar can also provide vertical  
53 distribution information for tropospheric  $O_3$  (Keckhut et al., 2004; Yang et al., 2023), there are very  
54 few routinely operating stations.

55 The principal sources of vertically-resolved, trend-quality observations of tropospheric  $O_3$  are  
56 therefore balloon-borne ozonesondes, and IAGOS aircraft observations. The World Ozone and  
57 Ultraviolet Radiation Data Centre (WOUDC) and the In-service Aircraft for a Global Observing  
58 System database (IAGOS) house the data from these two observation programs with the longest

59 duration and the most global stations, which are the most widely used for tropospheric O<sub>3</sub> studies  
60 (Gaudel et al., 2020; Liao et al., 2021; Tarasick et al., 2019; Wang et al., 2022; Zang et al., 2024).  
61 These two datasets are used to study the distribution, variability and trends of tropospheric O<sub>3</sub>, and  
62 its sources and transport, as well as satellite and model validation (Hu et al., 2017; Gaudel et al.,  
63 2018; 2020; Wang et al., 2022; Zhang et al., 2008). The first phase of the Tropospheric Ozone  
64 Assessment Report (TOAR-I), initiated in 2014, utilized available surface, ozonesonde, aircraft, and  
65 satellite observations to assess tropospheric O<sub>3</sub> trends from 1970 to 2014 (Schultz et al., 2017). Hu  
66 et al. (2017) found that the largest bias in a chemical transport model, GEOS-Chem, with respect to  
67 ozonesondes and IAGOS observations, is in high northern latitudes in winter-spring, where the  
68 simulated O<sub>3</sub> is 10-20 ppb lower. Wang et al. (2022) examined observed tropospheric O<sub>3</sub> trends,  
69 their attributions, and radiative impacts from 1995 to 2017, using aircraft observations from IAGOS,  
70 ozonesondes, and a multi-decadal GEOS-Chem chemical model simulation, and found increases in  
71 tropospheric O<sub>3</sub> (950-250 hPa) of  $2.7 \pm 1.7$  ppbv per decade from IAGOS observations in the  
72 Northern Hemisphere and at 19 of 27 global ozonesonde sites averaging  $1.9 \pm 1.7$  ppbv per decade.  
73 There are also a number of comparative studies on these two datasets (Zbinden et al., 2013; Staufer  
74 et al., 2013, 2014; Tanimoto et al., 2015; Tarasick et al., 2019). Staufer et al. (2013, 2014) used  
75 trajectory calculations to match air parcels sampled by both sondes and aircraft. Zbinden et al. (2013)  
76 compared coincidences ( $\pm 24$  hours) at three site pairs, while Tanimoto et al. (2015) examined  
77 simultaneous observations ( $\pm 3$  hours for sonde versus aircraft) at several site pairs less than 100 km  
78 apart. In general, these studies show small (6% or less) negative biases of aircraft measurements  
79 against ECC sondes. Tarasick et al. (2019) compared trajectory-mapped averages over 20°-70° N  
80 of ozonesonde and MOZAIC/IAGOS profiles and concluded that over 1994-2012 ozonesonde  
81 measurements were about  $5 \pm 1\%$  higher in the lower troposphere and  $8 \pm 1\%$  higher in the upper  
82 troposphere.

83 **As shown above, the global O<sub>3</sub> vertical distribution datasets observed by WOUDC and IAGOS have**  
84 **been widely used in various studies. Still, a long-term and multi-site systematic comparison of these**  
85 **two datasets is rare, especially for the observations in the past three decades.** In this study, we  
86 attempt to make the most comprehensive evaluation to date of the relative biases of IAGOS and  
87 sonde profiles, using as many station pairs as possible. We identify 23 suitable pairs of sites in the

88 WOUDC and IAGOS datasets from 1995 to 2021, compare the average vertical distribution of  
89 tropospheric O<sub>3</sub> shown by ozonesonde and aircraft measurements, and analyze their differences by  
90 ozonesonde type and by station-airport distance.

91

## 92 **2 Data and methods**

### 93 **2.1 MOZAIC-IAGOS observations**

94 The MOZAIC (Measurements of OZone and water vapor on Airbus In-service airCRAFT) program,  
95 initiated in 1994 and incorporated into the IAGOS (In-service Aircraft for a Global Observing  
96 System; [www.iagos.org](http://www.iagos.org)) program since 2011, takes advantage of commercial aircraft to provide  
97 worldwide in-situ measurements of several trace gases (e.g., O<sub>3</sub> and CO) and meteorological  
98 variables (e.g., water vapor) throughout the troposphere and the lower stratosphere (Marenco et al.,  
99 1998; Petzold et al., 2015; Nédélec et al., 2015). O<sub>3</sub> measurements are performed using a dual-beam  
100 UV-absorption monitor (time resolution of 4 seconds) with an instrumental uncertainty of  $\pm 2$   
101 ppbv+2% (Thouret et al., 1998; Blot et al., 2021). It should be noted that this is only the instrumental  
102 uncertainty, and does not include sampling uncertainties (possible losses) caused by the inlet line  
103 and the compressor before the UV-photometric measurements are made. Loss of O<sub>3</sub> on the inlet  
104 pump was an issue in earlier aircraft O<sub>3</sub> sampling programs (Brunner et al., 2001; Dias-Lalcaca et  
105 al., 1998; Schnadt Poberaj et al., 2007; Thouret et al., 2022), but Thouret et al. (1998) found it  
106 negligible for MOZAIC/IAGOS.

107 More details on the new IAGOS instrumentation can be found in Nédélec et al. (2015). The  
108 continuity of the dataset between the MOZAIC and IAGOS programs has been demonstrated based  
109 on their 2-year overlap (2011-2012) (Nédélec et al., 2015). **Blot et al. (2021) evaluated the internal  
110 consistency of the O<sub>3</sub> measurements since 1994, which confirmed the instrumental uncertainty of  
111  $\pm 2$  ppb. Moreover, they found no bias drift amongst the different instrument units (six O<sub>3</sub> IAGOS-  
112 MOZAIC instruments, nine IAGOS-Core Package1 and the two instruments used in the IAGOS-  
113 CARIBIC aircraft).**

### 114 **2.2 WOUDC ozonesonde observations**

115 The World Ozone and Ultraviolet Radiation Data Centre (WOUDC) is part of the Global  
116 Atmosphere Watch (GAW) program of the World Meteorological Organization

117 (<https://woudc.org/data/explore.php>). The WOUDC is operated by Environment and Climate  
118 Change Canada. WOUDC ozonesonde data have been evaluated in a number of WMO-sponsored  
119 international field intercomparisons (Attmannspacher and Dütsch, 1970, 1981; Kerr et al, 1994) and  
120 more recently in laboratory simulation chamber experiments using a standard reference photometer  
121 (Smit et al., 2007, 2024; Thompson et al., 2019). In the global ozonesonde network, while different  
122 ozonesonde types were common in the past, more than 95% of current sounding stations use  
123 electrochemical concentration cells (ECC). ECC ozonesondes have a precision of 3-5% ( $1-\sigma$ ) while  
124 the precision of other sonde types is somewhat poorer, at about 5–10% for Brewer-Mast and the  
125 Japanese KC (Carbon-Iodine) sonde, and somewhat larger for the Indian-sonde (Kerr et al., 1994;  
126 Smit et al., 2007). Biases with respect to UV reference spectrometers have been estimated for ECC  
127 sondes at 1-5% in the troposphere (Smit et al., 2021; Tarasick et al., 2019, 2021).

### 128 **2.3 Data processing**

129 The two datasets were first screened for airport-sonde station pairs within a latitude separation of  
130  $<4^\circ$  and a longitude separation of  $<4^\circ$ . Many sonde stations have observational records that do not  
131 overlap with the IAGOS period (1994-present). In addition, the IAGOS dataset has large gaps at  
132 many airports, because the frequency of visits to airports by aircraft that take part in IAGOS depends  
133 on commercial airlines' operating constraints. In total, 23 station pairs (Fig. 1) were identified with  
134 a separation of less than  $4^\circ$  in both latitude and longitude, and coincident observations over at least  
135 nine months. The majority of the 23 ozonesonde site records are ECC (17), while four are Indian-  
136 sonde, one Brewer-Mast, and one Carbon-Iodine (the Japanese KC sonde). These stations were  
137 divided into 3 groups according to the distance (D) between the ozonesonde station and the airport:  
138  $D < 1^\circ$ ,  $1^\circ < D < 2^\circ$ , and  $2^\circ < D < 4^\circ$ . Specific information on the comparison stations is shown in Table  
139 1.

140 The observation times of the ozonesonde and aircraft are generally not the same. Ozonesondes are  
141 typically launched once a week, although a few stations have more frequent launches. The aircraft  
142 records generally contain more frequent observations, but observation times vary. For the selected  
143 23 stations, we calculated the mean  $O_3$  vertical profiles at 1km resolution (the first layer is from the  
144 surface to 1 km above sea level) for each month during the observational period for the two datasets.  
145 A minimum of four aircraft profiles were required to estimate a monthly mean profile; because

146 ozonesonde launches are typically only a few times per month, no minimum was required to  
147 estimate a monthly mean profile. Only data with monthly means in both datasets were included for  
148 further analysis. Comparisons between the two datasets were made by ozonesonde type and by  
149 station-airport distance.

150

### 151 **3. Results and discussion**

#### 152 **3.1 Comparison of the vertical profiles of tropospheric O<sub>3</sub> from four types of ozonesondes and** 153 **aircraft observations**

154 Previous intercomparisons of sondes launched on the same balloon (Attmannspacher and Dütsch,  
155 1970, 1981; Beekmann et al, 1994, 1995; Deshler et al., 2008; Hilsenrath et al., 1986; Kerr et al,  
156 1994; Smit et al., 2007) have shown that sondes of different types respond somewhat differently to  
157 the same O<sub>3</sub> vertical profile; that is, they have relative biases, that vary with altitude. Fig. 2 therefore  
158 compares the mean vertical profiles of tropospheric O<sub>3</sub> from ozonesonde and aircraft measurements,  
159 separated by ozonesonde type. Both O<sub>3</sub> concentrations and absolute differences between  
160 ozonesonde and aircraft increase with altitude, especially above 9 km. **Average tropospheric O<sub>3</sub>**  
161 **profiles observed by ECC, Brewer-Mast, and Carbon-Iodine sondes are in good agreement with**  
162 **aircraft measurements, with biases of 2.58 ppb, -0.28 ppb and 0.67 ppb, while the agreement with**  
163 **the Indian-sonde is poorer, with a bias of 15.32 ppb.** The Indian-sonde average also shows a linear  
164 increase with altitude, while the aircraft measurements indicate an O<sub>3</sub> decrease with altitude above  
165 8 km (Fig. 2b). This behavior is most clearly related to the comparisons of stations 2°-4° apart in  
166 spring (Fig. S9).

167 **These results are broadly consistent with those from JOSIE 1996 (Smit et al. 1996; Smit and Kley,**  
168 **1998; Thompson et al., 2019), and with the northern hemisphere average result from Tarasick et al.**  
169 **(2019). (Their Figure 20b; note that it is largely based on ECC sondes, and the scale is inverted**  
170 **(IAGOS-sondes) from the sense we use here.)**

171 **Fig. 3 shows correlation plots of monthly mean O<sub>3</sub> at 1 km vertical intervals for months when both**  
172 **IAGOS and ozonesonde data are available at the same location. While these monthly averages are**  
173 **of data not necessarily coincident in time, Fig. 3 indicates that the data compare well on this**  
174 **timescale, with correlation coefficients (R) of 0.71, 0.88 and 0.66, respectively (Fig. 3a-3c). The**

175 agreement between the Indian-sonde and aircraft observations is poor, however, with an R of only  
176 0.44 (Fig. 3d). The RMSE of O<sub>3</sub> observed with the four types of ozonesondes (ECC, Brewer-Mast,  
177 Carbon-Iodine and Indian-sonde) and the aircraft is 15.99 ppb, 14.15 ppb, 16.26 ppb and 29.85 ppb,  
178 respectively. After calculation, we obtained the slopes and offsets of ECC, Brewer-mast, Carbon-  
179 iodine and Indian-sonde without forcing the fitted lines through zero, the slope is 0.71, 0.88, 0.56  
180 and 0.74, respectively, and the offset is 18.94 ppb, 6.89ppb, 27.48ppb and 27.84ppb. When we force  
181 the intercept to zero for the regressions, the slope is larger than the slope without forcing the fitted  
182 lines through zero (fig. 3). In generally, when O<sub>3</sub> is zero both the ozonesondes and the aircraft will  
183 measure zero. However, there is an offset in the fit of the two data sets due to potential causes for  
184 systematic differences during the observation measurement process, e.g., high background current  
185 in the sonde data.

186 Fig. 2 shows that the mean differences between ozonesonde and aircraft measurements vary  
187 significantly with altitude. This can also be observed clearly from the relative differences (RD),  
188 expressed as  $(O_{3\text{-ozonesonde}} - O_{3\text{-aircraft}}) / O_{3\text{-aircraft}} \times 100\%$  (Fig. 4). O<sub>3</sub> concentrations from ECC  
189 measurements are higher than those from aircraft measurements in all altitudes except at the surface.  
190 Mean O<sub>3</sub> concentrations reported by Brewer-Mast sondes are lower than those from IAGOS below  
191 7 km, but higher between 7 and 12 km. O<sub>3</sub> concentrations reported by Carbon-Iodine sondes are  
192 higher than those observed from aircrafts below 2 km, but significantly lower above 8 km. In relative  
193 terms, the bias between ECC sonde and aircraft measurements varies little with altitude, except near  
194 the ground. The mean relative bias for Brewer-Mast measurements is at an absolute maximum of -  
195 19 % near the ground, but increases slowly above 3 km, and is positive above 7 km, reaching more  
196 than +10 % at 10-11 km. The relative bias for Carbon-Iodine measurements is about 8% below 2  
197 km, becomes quite small from 2 - 8 km, and becomes large and negative above 8 km.  
198 The Indian-sonde observations show much larger mean differences from the aircraft measurements.  
199 Biases are everywhere positive, and as high as nearly 60% or 30 ppb, with much higher uncertainty  
200 (standard errors) at each altitude as well (Fig. 2b, Fig. 4).  
201 The region below 3 km has many local ozone sources and sinks (cities, airports, rural environment,  
202 etc). In comparison, the region above 8 km is significantly influenced by stratosphere-troposphere  
203 exchange, jet streams, and tropopause folds. Fig. S1 shows that the R between ozonesondes and

204 aircraft observations is higher near the ground (< 2 km) and at high altitudes (> 10 km). This shows  
205 that although the influencing factors of O<sub>3</sub> near the ground and at high altitudes are more complex,  
206 their long-term temporal variation characteristics are similar. The influences of cities, airports, rural  
207 environment, stratosphere-troposphere exchange, jet streams, tropopause folds, etc., have a more  
208 significant impact on the concentration of O<sub>3</sub> in the short term.

209 The correlation between four types of ozonesondes and aircraft observations also varies with altitude  
210 (Fig. S1). From 0-8 km, the correlation between ECC and aircraft observations decreases with  
211 altitude, with R being 0.71 at 0-1 km and reaching a minimum of 0.29 at 8-9 km; from 8-12 km, R  
212 increases with altitude, reaching 0.49 at 11-12 km. The correlation between the other three  
213 ozonesondes (Brewer-mast, Indian-sonde and Carbon-iodine) and the aircraft observations all vary  
214 with altitude, with different inflection points. The number of stations for these three types of  
215 ozonesondes is small (Table 1). Therefore, local variable influences on O<sub>3</sub> are more important, so  
216 R varies more with altitude.

217 The bias and RMSE with respect to the aircraft observations of the four types of ozonesondes at 8-  
218 12 km are higher than that at other altitudes. In contrast, the bias and RMSE values below 8 km are  
219 smaller and vary less with altitude, consistent with the vertical distribution characteristics of O<sub>3</sub>  
220 concentration in Fig. 2. This is likely due to the higher concentration of O<sub>3</sub> and the typically larger  
221 difference in spatial distance between ozonesonde and aircraft observations at 8-12km.

222 In addition, the bias and RMSE relative to the aircraft observations at different altitudes for ECC,  
223 Carbon-iodine and Brewer-mast sondes are lower than those for the Indian-sonde, which is similar  
224 to the results of the above analysis of O<sub>3</sub> concentration.

225 It should be noted that these comparisons only give an average relative bias between sondes and  
226 IAGOS. The true value of the ozone profile remains unknown, as do the absolute biases of sondes  
227 and IAGOS.

228

### 229 **3.2 Seasonal variations in relative biases between ozonesondes and IAGOS**

230 Fig. 5 compares mean profiles observed by ECC ozonesondes and IAGOS, separated by season.  
231 There are modest seasonal differences in the relative bias profiles, with somewhat larger average  
232 biases in winter and spring, but average biases are all positive (ECC sondes higher) and at all levels



233 the average seasonal biases are not statistically different.

234 The modest seasonal differences that are apparent in Fig. 5 and in Figs. S2-S4 are likely due to the  
235 modest sample size (for ECC sondes) and small sample sizes (for other types). The actual  
236 coincidence in time for profiles can range from less than one day to about 1-3 weeks, depending on  
237 the number of ozonesonde and aircraft O<sub>3</sub> profiles collected within each month-bin. This means the  
238 larger the atmospheric variability of O<sub>3</sub> is, the larger the real differences between ozonesonde and  
239 aircraft O<sub>3</sub> can become, particularly when the number of profiles within a month-bin are small. In  
240 addition, there are errors due to variations in the aircraft take-off and landing trajectories and the  
241 balloon rise rate, the geographical location of the observation stations (and any associated  
242 meteorological differences) and any systematic difference in standard observational times.

243 Table 2 indicates that in all four seasons ECC data correlate well with aircraft observations, with R  
244 ranging from 0.71 to 0.76, but with larger average biases in winter and spring, as noted. It is not  
245 clear if these seasonal average differences in bias are significant, as the uncertainty ranges on the  
246 seasonal averages (lower plot of Fig. 5) overlap.

247 The vertical distribution of tropospheric O<sub>3</sub> observed by Brewer-Mast and IAGOS aircraft in the  
248 four seasons is similar (Fig. S2). Differences are also similar, except above 7 km, where the  
249 uncertainties are larger, and in general the uncertainty ranges on the seasonal difference averages  
250 overlap. Since these comparisons come from only one station pair, some of the differences may be  
251 attributable to local differences in topography and meteorology. Table 2 shows that correlations for  
252 the ensemble of Brewer-Mast stations are higher than those for ECC stations. Like the ECC sondes,  
253 average biases are all positive, but this is determined by the biases above 7 km (Fig. 4); unlike the  
254 ECCs, biases are negative in the lowest 3 km.

255 The vertical distribution of tropospheric O<sub>3</sub> concentrations observed by Carbon-Iodine sondes and  
256 IAGOS aircraft in the four seasons are similar, except in summer when the tropopause is high (Fig.  
257 S3). The difference plots are fairly similar, except in the lowest 3 km, where differences become  
258 quite large in summer. Like the previous comparison for Brewer-Mast sondes, these comparisons  
259 come from only one station pair, and so the large differences in the boundary layer in summer are  
260 likely due to local O<sub>3</sub> production sampled by the sonde but not the aircraft. Likely for this reason,  
261 the consistency between Carbon-Iodine and aircraft observations is poor in summer, with R being

262 only 0.46 (Table 2). For the other three seasons it is fairly good.  
263 The tropospheric O<sub>3</sub> observed by Indian-sondes displays a consistently high bias relative to IAGOS  
264 in all seasons, and the seasonal difference plots are quite similar, except in the lowest 3 km in winter  
265 (Fig. S4). This different behavior in winter is likely due to local ozone production sampled by the  
266 aircraft but not the sonde. Temperature inversions are common in the winter in northern India and  
267 trap local pollution. The very low values registered by the aircraft near the surface in summer also  
268 suggest local effects, in this case titration by NO<sub>x</sub>.

269 The tropospheric O<sub>3</sub> observed by Indian-sonde in the four seasons is 43.3-79.4 ppb, 31.4-80.2 ppb,  
270 42.2-69.6 ppb and 51.5-87.5 ppb, and that observed by aircraft in the four seasons is 22.8-60.1 ppb,  
271 14.8-47.1 ppb, 25.0-44.1 ppb and 35.6-53.3 ppb (Fig. S4). The tropospheric O<sub>3</sub> observed in Indian-  
272 sonde in the four seasons increases with height almost linearly. The tropospheric O<sub>3</sub> observed by  
273 aircraft first increases and then decreases with altitude in spring, summer and autumn, while in  
274 winter, it first decreases and then increases with altitude. The tropospheric O<sub>3</sub> observed by the  
275 Indian-sonde and the aircraft is quite different, and the RD in the four seasons is 6.3% to 47.5%,  
276 22.6% to 52.9%, 26.4% to 40.6% and 5.13% to 39.13%. Table 2 indicates poor consistency between  
277 Indian-sonde and aircraft observations in all four seasons, with R in winter only 0.18. The bias and  
278 RMSE in winter are the largest, at 40.07 ppb and 64.99 ppb. The bias, R and RMSE in the other  
279 three seasons are smaller, and the differences between them slight.

### 280 **3.3 Dependence of relative biases on station-airport distances**

281 A major concern with comparing IAGOS and ozonesonde observations is that the stations and  
282 airports are not generally co-located, and even where they are close, the flight paths taken by balloon  
283 and aircraft are quite different. Fig. 6 compares the average vertical distribution of tropospheric O<sub>3</sub>  
284 observed at different station-airport distances by ECC sondes and IAGOS aircraft. Note that we  
285 continue to separate sonde station data by type --- only ECC data are used here. Sonde-aircraft pairs  
286 have been grouped by station-airport distance (Table 1). The differences in average bias vary only  
287 very modestly between the different station-airport distance categories, and those differences are  
288 not statistically different at the 95% confidence level (Fig. 6d). This, partially owing presumably to  
289 the use of mean monthly averages, is encouraging, as this provides further evidence that the average  
290 bias we have derived is an artifact strictly of instrument differences.

291 Table 3 indicates that the bias variation between ECC and aircraft observations at different station-  
292 airport distances is small, ranging from 5.7 ppb to 9.8 ppb. Correlations for these groupings are also  
293 fairly similar, at  $R = 0.8, 0.9$  and  $0.7$ .

294 Compared with ECC sondes, the consistency between the Indian-sonde and aircraft observations is  
295 poor at all station-airport distances, with much larger biases, and poor correlations, with  $R = 0.2$  to  
296  $0.4$ . Nevertheless, Fig. S5 shows that the profiles of average differences are quite similar for station-  
297 airport distances  $< 1^\circ$ , and distances of  $2^\circ$ - $4^\circ$  (Fig. S5c).

298 Fig. 7 and Figs. S6-S8 examine possible seasonal variation in the differences at different station-  
299 airport distances, for ECC sondes. The mean differences for the different station-airport distance  
300 categories are larger than for the annual averages (Fig. 6), but in general those differences are not  
301 statistically different at the 95% confidence level (Figs. 7d and S6d-S8d).

302

### 303 **3.4 Comparison of ozonesonde relative biases under operational conditions using IAGOS** 304 **observations as a transfer standard**

305 The foregoing discussion demonstrates that, consistent with previous work, there is a fairly constant  
306 relative bias between IAGOS and sondes, with considerable dependence on sonde type, as expected  
307 from previous sonde intercomparisons like JOSIE 1996. Although uncertainties are sizeable due to  
308 the relatively sparse nature of the available data, we find consistent differences at all sites, with little  
309 dependence on season or on station-airport separation, and little regional dependence (not shown).  
310 Notwithstanding this overall sonde-IAGOS bias, we can use these station-airport comparisons to  
311 derive relative biases of the different sonde types in use in the global network.

312 This does not assume that the aircraft data are unbiased. The true value of the  $O_3$  profile (or even its  
313 average) remains unknown, as do the absolute biases of sondes and IAGOS. It does assume:

- 314 1. That the measurement errors are random and normally distributed;
- 315 2. That there is one, constant bias for each measurement type (that is, if, for example, the Indian  
316 sonde has changed over the period of comparison, or the IAGOS instruments have different biases,  
317 there would be additional error that is not included in our uncertainty estimate);
- 318 3. That the measurement biases are not dependent on the geographic location or other variability of  
319 the  $O_3$  profile. This does not assume that the average  $O_3$  profile is the same, just that the instruments

320 respond in the same way.  
321 With these assumptions we can use the results of Fig. 2 to estimate the relative biases of each sonde  
322 type to each other. The uncertainty of the comparisons will be the quadratic sum of the uncertainties  
323 of the two IAGOS-sonde comparisons. The results are shown in Table 4. This intercomparison of  
324 the different sonde types has an important advantage: it compares ozonesonde relative biases under  
325 operational conditions, as it compares the data that are actually in databases like the WOUDC. It  
326 also fills a gap, as the last WMO international intercomparison involving all four sonde types was  
327 JOSIE 1996. These results are broadly consistent with those from JOSIE 1996 (Smit and Kley, 1998;  
328 their Table 8 and Fig. 11).

329 In fact, the types of ozonesonde have changed during long-term observations at some stations (e.g.  
330 Uccle and Payerne). De Backer et al. (1998) showed that with the use of an appropriate correction  
331 procedure, accounting for the loss of pump efficiency with decreasing pressure and temperature, it  
332 is possible to reduce the mean difference between O<sub>3</sub> profiles obtained with both types of sondes  
333 below 3%, which is statistically insignificant over nearly the whole operational altitude range (from  
334 the ground to 32 km). Stübi et al. (2008) also found that the O<sub>3</sub> difference between the Brewer-Mast  
335 and the ECC ozonesonde data shows good agreement between the two sonde types, and the profile  
336 of the O<sub>3</sub> difference is limited to ±5% (±0.3 mPa) from the ground to 32 km. The results for Brewer-  
337 Mast sondes in Table 4 should also be applicable to the older Payerne and Uccle records, and are  
338 generally consistent with these results and with those for the older Canadian records (Tarasick et al.,  
339 2002; 2016).

340 The results in Table 4 will be quite valuable for addressing the problem of relative biases when  
341 merging ozonesonde data into global climatologies (e.g. McPeters et al., 2007; McPeters and Labow,  
342 2012; Bodeker et al., 2013; Liu et al., 2013; Hassler et al., 2018;).

#### 343 **4 Conclusions**

344 The vertical distribution of tropospheric O<sub>3</sub> observed by ozonesondes and IAGOS aircraft sensors  
345 are compared at 23 pairs of sites between about 30°S and 55°N from 1995 to 2021. Overall, ECC,  
346 Brewer-Mast, and Carbon-Iodine sondes agree reasonably well with aircraft observations, with  
347 average biases of 2.58 ppb, -0.28 ppb, and 0.67 ppb, and correlation coefficients of 0.72, 0.82, and  
348 0.66, respectively. The agreement between the aircraft and Indian-sonde observations is poor, with

349 an average bias of 15.32 ppb and R of 0.44. Ozonesondes and aircraft observations have smaller R  
350 in the middle troposphere, but larger bias and RMSE in the upper troposphere. The bias and RMSE  
351 relative to the aircraft observations at different altitudes for ECC, Carbon-iodine and Brewer-mast  
352 sondes are lower than those for the Indian-sonde.

353 Notwithstanding this general agreement, all sonde types show significant average biases with  
354 respect to IAGOS. The O<sub>3</sub> concentration observed by ECC sondes is on average higher by 5-10%  
355 than that observed by IAGOS aircraft, and the relative bias increases modestly with altitude.  
356 Seasonal variations in the relative bias are not in general statistically significant. The distance  
357 between station and airport within 4° also has little effect on the comparison results. When the ECC  
358 station pairs are grouped by station-airport distances of <1° (latitude and longitude), 1-2°, and 2-4°,  
359 biases with respect to IAGOS measurements vary from 5.7 to 9.8 ppb, and correlations from 0.7 to  
360 0.9.

361 Thus, the observed average relative bias between sondes and IAGOS found in this study, also noted  
362 by previous authors (Zbinden et al., 2013; Staufer et al., 2013, 2014; Tanimoto et al., 2015; Tarasick  
363 et al., 2019), is a robust result. Possible reasons for the difference include: side reactions that cause  
364 sondes to produce excess iodine (Saltzman and Gilbert, 1959), and/or loss of O<sub>3</sub> on the inlet pump  
365 that could cause IAGOS monitors to read low at pressures below 800 hPa. The latter was an issue  
366 in earlier aircraft O<sub>3</sub> sampling programs (Schnadt Poberaj et al., 2007; Dias-Lalcaca et al., 1998;  
367 Brunner et al., 2001), but Thouret et al. (1998) found it negligible for MOZAIC/IAGOS. A recent  
368 intercomparison campaign at the World Calibration Centre for Ozone Sondes (WCCOS) in Julich  
369 in June 2023 indicates that the pumps do not greatly influence the ozone IAGOS measurements  
370 between 1000 and 200 hPa. The IAGOS-CORE O<sub>3</sub> measurements (Package 1 with pressurization  
371 pumps) and IAGOS-CARIBIC O<sub>3</sub> measurements differ by less than 2%, and the WCCOS reference  
372 UV photometer measurements are usually higher by 1-2% (to a maximum of 5%) compared to both  
373 IAGOS instruments (Blot et al., 2021; Nédélec et al., 2015; Thouret et al., 2022). IAGOS-CARIBIC  
374 does not have pressurization system, so that's why the good comparison between both IAGOS  
375 systems means a lot.

376 However, as noted by Saltzman and Gilbert (1959), the differences in stoichiometry found at  
377 different pH values imply that the chemistry of reaction of O<sub>3</sub> with KI is complex, involving

378 reactions that cause loss of iodine, as well as reactions other than the principal one that produce  
379 additional iodine. Several authors have noted the existence of slow side reactions involving the  
380 phosphate buffer, with a time constant of about 20 minutes, that may also increase the stoichiometry  
381 from 1.0 (Tarasick et al., 2021, Smit et al., 2024). Furthermore, evaporation causes the concentration  
382 of the sensing solution to increase, which can further enhance the stoichiometry, by concentrating  
383 the phosphate buffer, and to a lesser degree, by increasing the concentration of the KI itself (Johnson  
384 et al., 2002). These factors could contribute to the observed average relative bias between sondes  
385 and IAGOS found in this study.

386 This result implies that care must be taken when merging ozonesonde and IAGOS measurement  
387 datasets. While the aircraft and sonde measurements are often complementary, filling in important  
388 spatial gaps that would otherwise exist if only one type were used, the records are not typically over  
389 the same period, and so merging can introduce spurious jumps if relative biases are not taken into  
390 account.

391 The importance of O<sub>3</sub> in the troposphere as an air pollutant and a greenhouse gas, and therefore of  
392 accurate measurements of its temporal and spatial distribution implies that it will be important to  
393 resolve the causes of this bias, and so further research involving more direct comparisons of IAGOS  
394 instrumentation and ozonesondes, e.g. in the WCCOS chamber, are strongly recommended.

395 These results are also useful to evaluate the relative biases of the different sonde types in the  
396 troposphere, using the aircraft as a transfer standard. This intercomparison of the different sonde  
397 types has the advantage that it compares ozonesonde relative biases under operational conditions;  
398 that is, the data that are actually in databases like the WOUDC. These results will be invaluable for  
399 addressing relative biases when merging ozonesonde data into global climatologies (e.g. Bodeker  
400 et al., 2013; Hassler et al., 2018; Liu et al., 2013; McPeters et al., 2007; McPeters and Labow, 2012).

401

402 **Competing interests.** The contact authors have declared that none of the authors has any competing  
403 interests.

404 **Data availability.** The global ozone sounding data were acquired from the World Ozone and  
405 Ultraviolet Radiation Data Center (<http://www.woudc.org>) operated by Environment Canada. The  
406 IAGOS data are created with support from the European Commission, national agencies in Germany

407 (BMBF), France (MESR), and the UK (NERC), and the IAGOS member institutions  
408 (<http://www.iagos.org/partners>).

409 **Author contributions.** **HW:** Data curation, Methodology, Validation, Visualization, Writing -  
410 original draft preparation, Writing - review & editing, Funding acquisition. **LS:** Methodology,  
411 Investigation, Writing - original draft. **DWT:** Data curation, Resources, Conceptualization,  
412 Supervision, Writing - original draft preparation, Writing - review & editing. **JL:** Data curation,  
413 Resources, Methodology, Conceptualization, Supervision, Writing - original draft preparation,  
414 Writing - review & editing, Funding acquisition. **TZ:** Funding acquisition, Writing - review &  
415 editing. **HGJS** and **RVM:** Writing - review & editing. **HGJS** and **RB:** Acquisition of IAGOS data,  
416 Quality assessment IAGOS data.

417

418 **Acknowledgments.** We thank many whose dedication makes datasets used in this study possible.  
419 The global O<sub>3</sub> sounding data were acquired from the World Ozone and Ultraviolet Radiation Data  
420 Center (<http://www.woudc.org>) operated by Environment Canada, Toronto, Canada, under the  
421 auspices of the World Meteorological Organization. Flight-based atmospheric chemical  
422 measurements are from IAGOS. IAGOS is funded by the European Union projects IAGOS-DS and  
423 IAGOS-ERI. The IAGOS data are created with support from the European Commission, national  
424 agencies in Germany (BMBF), France (MESR), and the UK (NERC), and the IAGOS member  
425 institutions (<http://www.iagos.org/partners>). The participating airlines (Lufthansa, Air France,  
426 Austrian, China Airlines, Iberia, Cathay Pacific, Air Namibia, Sabena) supported IAGOS by  
427 carrying the measurement equipment free of charge since 1994. We are also thankful to the Digital  
428 Research Alliance of Canada at the University of Toronto for facilitating data analysis.

429

430 **Financial support.** This study was supported by the Natural Science and Engineering Council of  
431 Canada (Grant No. RGPIN-2020-05163), the National Key Research and Development Program of  
432 China (Grant No., 2022YFC3701204), the National Natural Science Foundation of China  
433 (42275196 and 41830965), the Natural Science Foundation of Jiangsu Province (BK20231300), and  
434 Wuxi University Research Start-up Fund for Introduced Talents (2023r035).

435

436 **References**

- 437 Attmannspacher, A., and Dütsch, H.U., 1970. International ozone sonde intercomparison at the  
438 Observatory Hohenpeissenberg, Ber. Dtsch. Wetterdienstes, 120, 1-85.
- 439 Attmannspacher, A., and Dütsch, H.U., 1981. Second international ozone sonde intercomparison at  
440 the Observatory Hohenpeissenberg, Ber. Dtsch. Wetterdienstes, 157, 1-64.
- 441 Beekmann, M., Ancellet, G., Megie, G., Smit, H.G.J., Kley, D., 1994. Intercomparison campaign of  
442 vertical ozone profiles including electrochemical sondes of ECC and Brewer-Mast type and a  
443 ground based UV-differential absorption lidar. *Journal of Atmospheric Chemistry*, 19, 259-288.  
444 19.
- 445 Beekmann, M., Ancellet, G., Martin, D., Abonnel, C., Duverneuil, G., Eideliman, F., Bessemoulin,  
446 P., Fritz, N., Gizard, E., 1995. Intercomparison of tropospheric ozone profiles obtained by  
447 electrochemical sondes, a ground based lidar and an airborne UV-photometer. *Atmospheric  
448 Environment*, 29(9), 1027-1042.
- 449 Bernhard, G.H., Bais, A.F., Aucamp, P.J., Klekociuk, A.R., Liley, J.B., McKenzie, R.L., 2023.  
450 Stratospheric ozone, UV radiation, and climate interactions. *Photochemical and  
451 Photobiological Sciences*, 1-53.
- 452 Blot, R., Nedelec, P., Boulanger, D., Wolff, P., Sauvage, B., Cousin, J.-M., Athier, G., Zahn, A.,  
453 Obersteiner, F., Scharffe, D., Petetin, H., Bennouna, Y., Clark, H., Thouret, V., 2021. Internal  
454 consistency of the IAGOS ozone and carbon monoxide measurements for the last 25 years.  
455 *Atmospheric Measurement Techniques*, 14, 3935-3951, [https://doi.org/10.5194/amt-14-3935-  
456 2021](https://doi.org/10.5194/amt-14-3935-2021).
- 457 Bodeker, G. E., Hassler, B., Young, P. J., Portmann, R. W., 2013. A vertically resolved, global, gap-  
458 free ozone database for assessing or constraining global climate model simulations. *Earth  
459 System Science Data*, 5, 31-43, <https://doi.org/10.5194/essd-5-31-2013>.
- 460 Brunner, D., J. Staehelin, D. Jeker, H., Wernli, U. Schumann, 2001. Nitrogen oxides and ozone in  
461 the tropopause region of the Northern Hemisphere: Measurements from commercial aircraft in  
462 1995/96 and 1997. *Journal of Geophysical Research: Atmospheres*, 106, 27673-27699.
- 463 Callis, L.B., Boughner, R.E., Natarajan, M., Lambeth, J.D., Baker, D.N., Blake, J.B., 1991. Ozone  
464 depletion in the high latitude lower stratosphere: 1979-1990. *Journal of Geophysical Research*:



465 Atmospheres, 96(D2), 2921-2937.

466 David, L.M. and Nair, P.R., 2013. Tropospheric column O<sub>3</sub> and NO<sub>2</sub> over the Indian region observed  
467 by Ozone Monitoring Instrument (OMI): Seasonal changes and long-term trends. Atmospheric  
468 Environment, 65, 25-39.

469 De Backer, H., De Muer, D., De Saelaer, G., 1998. Comparison of ozone profiles obtained with  
470 Brewer-Mast and Z-ECC sensors during simultaneous ascents. Journal of Geophysical  
471 Research: Atmospheres, 103(D16), 19641-19648.

472 Deshler, T., Mercer, J.L., Smit, H.G., Stubi, R., Levrat, G., Johnson, B.J., Oltmans, S.J., Kivi, R.,  
473 Thompson, A.M., Witte, J., Davies, J., 2008. Atmospheric comparison of electrochemical cell  
474 ozonesondes from different manufacturers, and with different cathode solution strengths: The  
475 Balloon Experiment on Standards for Ozonesondes. Journal of Geophysical Research:  
476 Atmospheres, 113(D4), D04307, doi:10.1029/2007JD008975.

477 Dias-Lalcaca, P., Brunner, D., Imfeld, W., Moser, W., Staehelin, J., 1998. An automated system for  
478 the measurement of nitrogen oxides and ozone concentrations from a passenger aircraft:  
479 Instrumentation and first results of the NOXAR project. Environmental Science and  
480 Technology, 32(20), 3228-3236.

481 Ebojio, F., Burrows, J.P., Gebhardt, C., Ladstätter-Weißmayer, A., Von Savigny, C., Rozanov, A.,  
482 Weber, M., Bovensmann, H., 2016. Global tropospheric ozone variations from 2003 to 2011  
483 as seen by SCIAMACHY. Atmospheric Chemistry and Physics, 16(2), 417-436.

484 Fu, Y. and Tai, A.P.K., 2015. Impact of climate and land cover changes on tropospheric ozone air  
485 quality and public health in East Asia between 1980 and 2010. Atmospheric Chemistry and  
486 Physics, 15(17), 10093-10106.

487 García, O.E., Sanromá, E., Schneider, M., Hase, F., León-Luis, S.F., Blumenstock, T., Sepúlveda,  
488 E., Redondas, A., Carreño, V., Torres, C., Prats, N., 2022. Improved ozone monitoring by  
489 ground-based FTIR spectrometry. Atmospheric Measurement Techniques, 15(8), 2557-2577.

490 García, O.E., Schneider, M., Sepúlveda, E., Hase, F., Blumenstock, T., Cuevas, E., Ramos, R., Gross,  
491 J., Barthlott, S., Röhlings, A.N., Sanromá, E., 2021. Twenty years of ground-based NDACC  
492 FTIR spectrometry at Izaña Observatory-overview and long-term comparison to other  
493 techniques. Atmospheric Chemistry and Physics, 21(20), 15519-15554.

494 Gaudel, A., Cooper, O.R., Ancellet, G., Barret, B., Boynard, A., Burrows, J.P., Clerbaux, C., Coheur,  
495 P.F., Cuesta, J., Cuevas, E., Doniki, S., 2018. Tropospheric Ozone Assessment Report: Present-  
496 day distribution and trends of tropospheric ozone relevant to climate and global atmospheric  
497 chemistry model evaluation. *Elementa: Science of the Anthropocene*, 6.

498 Gaudel, A., Cooper, O.R., Chang, K.L., Bourgeois, I., Ziemke, J.R., Strode, S.A., Oman, L.D.,  
499 Sellitto, P., Nédélec, P., Blot, R., Thouret, V., 2020. Aircraft observations since the 1990s reveal  
500 increases of tropospheric ozone at multiple locations across the Northern Hemisphere. *Science*  
501 *Advances*, 6(34), eaba8272.

502 Gebhardt, C., Rozanov, A., Hommel, R., Weber, M., Bovensmann, H., Burrows, J.P., Degenstein,  
503 D., Froidevaux, L., Thompson, A.M., 2014. Stratospheric ozone trends and variability as seen  
504 by SCIAMACHY from 2002 to 2012. *Atmospheric Chemistry and Physics*, 14(2), 831-846.

505 Hassler, B., Kremser, S., Bodeker, G. E., Lewis, J., Nesbit, K., Davis, S. M., Chipperfield, M. P.,  
506 Dhomse, S. S., Dameris, M., 2018, An updated version of a gap-free monthly mean zonal mean  
507 ozone database. *Earth System Science Data*, 10, 1473-1490.

508 Hegarty, J., Mao, H., Talbot, R., 2009. Synoptic influences on springtime tropospheric O<sub>3</sub> and CO  
509 over the North American export region observed by TES. *Atmospheric Chemistry and*  
510 *Physics*, 9(11), 3755-3776.

511 Hilsenrath, E., Attmannspacher, W., Bass, A., Evans, W., Hagemeyer, R., Barnes, R., Komhyr, W.,  
512 Mauersberger, K., Mentall, J., Proffitt, M., Robbins, D., 1986. Results from the balloon ozone  
513 intercomparison campaign (BOIC). *Journal of Geophysical Research: Atmospheres*, 91(D12),  
514 13137-13152.

515 Hoogen, R., Rozanov, V.V., Burrows, J.P., 1999. Ozone profiles from GOME satellite data:  
516 Algorithm description and first validation. *Journal of Geophysical Research:*  
517 *Atmospheres*, 104(D7), 8263-8280.

518 Hu, L., Jacob, D.J., Liu, X., Zhang, Y., Zhang, L., Kim, P.S., Sulprizio, M.P., Yantosca, R.M., 2017.  
519 Global budget of tropospheric ozone: Evaluating recent model advances with satellite (OMI),  
520 aircraft (IAGOS), and ozonesonde observations. *Atmospheric Environment*, 167, 323-334.

521 Hubert, D., Heue, K.P., Lambert, J.C., Verhoelst, T., Allaart, M., Compernelle, S., Cullis, P.D., Dehn,  
522 A., Félix, C., Johnson, B.J., Keppens, A., 2021. TROPOMI tropospheric ozone column data:

523 geophysical assessment and comparison to ozonesondes, GOME-2B and OMI. *Atmospheric*  
524 *Measurement Techniques*, 14(12), 7405-7433.

525 Johnson, B.J., Oltmans, S.J., Vömel, H., Smit, H.G.J., Deshler, T., Kroeger, C., 2002. ECC  
526 Ozonesonde pump efficiency measurements and tests on the sensitivity to ozone of buffered  
527 and unbuffered ECC sensor cathode solutions. *Journal of Geophysical Research: Atmospheres*,  
528 107(4393), 10-1029. doi: 10.1029/2001JD000557.

529 Keckhut, P., McDermid, S., Swart, D., McGee, T., Godin-Beekmann, S., Adriani, A., Barnes, J.,  
530 Baray, J.L., Bencherif, H., Claude, H., di Sarra, A.G., 2004. Review of ozone and temperature  
531 lidar validations performed within the framework of the Network for the Detection of  
532 Stratospheric Change. *Journal of Environmental Monitoring*, 6(9), 721-733.

533 Kerr, J.B., Fast, H., McElroy, C.T., Oltmans, S.J., Lathrop, J.A., Kyro, E., Paukkunen, A., Claude,  
534 H., Köhler, U., Sreedharan, C.R., Takao, T., 1994. The 1991 WMO international ozonesonde  
535 intercomparison at Vanscoy, Canada. *Atmosphere-Ocean*, 32(4), 685-716.

536 Lefohn, A.S., Malley, C.S., Smith, L., Wells, B., Hazucha, M., Simon, H., Naik, V., Mills, G.,  
537 Schultz, M.G., Paoletti, E., De Marco, A., 2018. Tropospheric ozone assessment report: Global  
538 ozone metrics for climate change, human health, and crop/ecosystem research. *Elementa:*  
539 *Science of the Anthropocene*, 6.

540 Li, K., Jacob, D.J., Liao, H., Qiu, Y., Shen, L., Zhai, S., Bates, K.H., Sulprizio, M.P., Song, S., Lu,  
541 X., Zhang, Q., 2021. Ozone pollution in the North China Plain spreading into the late-winter  
542 haze season. *Proceedings of the National Academy of Sciences*, 118(10), e2015797118.

543 Li, K., Jacob, D.J., Shen, L., Lu, X., De Smedt, I., Liao, H., 2020. Increases in surface ozone  
544 pollution in China from 2013 to 2019: anthropogenic and meteorological  
545 influences. *Atmospheric Chemistry and Physics*, 20(19), 11423-11433.

546 Liao, Z., Ling, Z., Gao, M., Sun, J., Zhao, W., Ma, P., Quan, J., Fan, S., 2021. Tropospheric ozone  
547 variability over Hong Kong based on recent 20 years (2000-2019) ozonesonde  
548 observation. *Journal of Geophysical Research: Atmospheres*, 126(3), e2020JD033054.

549 Liu, G., Liu, J., Tarasick, D.W., Fioletov, V.E., Jin, J.J., Moeini, O., Liu, X., Sioris, C.E., Osman,  
550 M., 2013. A global tropospheric ozone climatology from trajectory-mapped ozone soundings.  
551 *Atmospheric Chemistry and Physics*, 13(21), 10659-10675.

552 Logan, J.A., 1985. Tropospheric ozone: Seasonal behavior, trends, and anthropogenic  
553 influence. *Journal of Geophysical Research: Atmospheres*, 90(D6), 10463-10482.

554 Ma, Y., Ma, B., Jiao, H., Zhang, Y., Xin, J., Yu, Z., 2020. An analysis of the effects of weather and  
555 air pollution on tropospheric ozone using a generalized additive model in Western China:  
556 Lanzhou, Gansu. *Atmospheric Environment*, 224, 117342.

557 McPeters, R.D., Labow, G.J., Logan, J.A., 2007. Ozone climatological profiles for satellite retrieval  
558 algorithms. *Journal of Geophysical Research: Atmospheres*, 112(D5), D05308.  
559 doi:10.1029/2005JD006823.

560 McPeters, R.D. and Labow, G.J., 2012. Climatology 2011: An MLS and sonde derived ozone  
561 climatology for satellite retrieval algorithms. *Journal of Geophysical Research: Atmospheres*,  
562 117(D10), D10303. doi:10.1029/2011JD017006.

563 Miles, G.M., Siddans, R., Kerridge, B.J., Latter, B.G., Richards, N.A.D., 2015. Tropospheric ozone  
564 and ozone profiles retrieved from GOME-2 and their validation. *Atmospheric Measurement  
565 Techniques*, 8(1), 385-398.

566 Meng, K., Zhao, T., Xu, X., Zhang, Z., Bai, Y., Hu, Y., Zhao, Y., Zhang, X., Xin, Y., 2022. Influence  
567 of stratosphere-to-troposphere transport on summertime surface O<sub>3</sub> changes in North China  
568 Plain in 2019. *Atmospheric Research*, 276, 106271.

569 Monks, P.S., Archibald, A.T., Colette, A., Cooper, O., Coyle, M., Derwent, R., Fowler, D., Granier,  
570 C., Law, K.S., Mills, G.E., Stevenson, D.S., 2015. Tropospheric ozone and its precursors from  
571 the urban to the global scale from air quality to short-lived climate forcer. *Atmospheric  
572 Chemistry and Physics*, 15(15), 8889-8973.

573 Nédélec, P., Blot, R., Boulanger, D., Athier, G., Cousin, J.M., Gautron, B., Petzold, A., Volz-Thomas,  
574 A., Thouret, V., 2015. Instrumentation on commercial aircraft for monitoring the atmospheric  
575 composition on a global scale: the IAGOS system, technical overview of ozone and carbon  
576 monoxide measurements. *Tellus B: Chemical and Physical Meteorology*, 67(1), 27791.  
577 <https://doi.org/10.3402/tellusb.v67.27791@zelb20.2016.68.issue-s1>

578 Percy, K.E., Legge, A.H., Krupa, S.V., 2003. Tropospheric ozone: a continuing threat to global  
579 forests? *Developments in Environmental Science*, 3, 85-118.

580 Perlwitz, J., Pawson, S., Fogt, R.L., Nielsen, J.E., Neff, W.D., 2008. Impact of stratospheric ozone

581 hole recovery on Antarctic climate. *Geophysical Research Letters*, 35(8).  
582 <https://doi.org/10.1029/2008GL033317>.

583 Ramanathan, V., Cicerone, R.J., Singh, H.B., Kiehl, J.T., 1985. Trace gas trends and their potential  
584 role in climate change. *Journal of Geophysical Research: Atmospheres*, 90(D3), 5547-5566.

585 Saltzman, B.E. and Gilbert, N., 1959. Iodometric microdetermination of organic oxidants and ozone.  
586 Resolution of mixtures by kinetic colorimetry. *Analytical Chemistry*, 31(11), 1914-1920.

587 Schnadt Poberaj, C., Staehelin, J., Brunner, D., Thouret, V., Mohnen, V., 2007. A UT/LS ozone  
588 climatology of the nineteen seventies deduced from the GASP aircraft measurement program.  
589 *Atmospheric Chemistry and Physics*, 7(22), 5917-5936.

590 Schultz, M.G., Schröder, S., Lyapina, O., Cooper, O.R., Galbally, I., Petropavlovskikh, I., Von  
591 Schneidmesser, E., Tanimoto, H., Elshorbany, Y., Naja, M., Seguel, R.J., 2017. Tropospheric  
592 Ozone Assessment Report: Database and metrics data of global surface ozone  
593 observations. *Elementa: Science of the Anthropocene*, 5.

594 Sharma, S., Sharma, P., Khare, M., 2017. Photo-chemical transport modelling of tropospheric ozone:  
595 A review. *Atmospheric Environment*, 159, 34-54.

596 Smit, H.G.J., Sträter, W., Helten, M., Kley, D., Ciupa, D., Claude, H.J., Köhler, U., Hoegger, B.,  
597 Levrat, G., Johnson, B., Oltmans, S.J., Kerr, J.B., Tarasick, D.W., Davies, J., Shitamichi, M.,  
598 Srivastav, S.K., Vialle, C., 1996. JOSIE: The 1996 WMO international intercomparison of  
599 ozonesondes under quasi-flight conditions in the environmental chamber at Jülich, *Proc.*  
600 *Quadrennial Ozone Symposium 1996, l'Aquila, Italy*, edited by R. D. Bojkov and G. Visconti,  
601 pp. 971-974, Parco Sci. e Tecnol. d'Abruzzo, Italy, 1996.

602 Smit, H.G., Straeter, W., Johnson, B.J., Oltmans, S.J., Davies, J., Tarasick, D.W., Hoegger, B., Stubi,  
603 R., Schmidlin, F.J., Northam, T., Thompson, A.M., 2007. Assessment of the performance of  
604 ECC-ozonesondes under quasi-flight conditions in the environmental simulation chamber:  
605 Insights from the Juelich Ozone Sonde Intercomparison Experiment (JOSIE). *Journal of*  
606 *Geophysical Research: Atmospheres*, 112(D19), D19306, doi:10.1029/2006JD007308.

607 Smit, H.G.J., 2014. Ozonesondes, in *Encyclopedia of Atmospheric Sciences*, Second Edition, edited  
608 by G.R. North, J.A. Pyle, and F. Zhang, Vol 1, pp. 372–378, Academic Press, London.

609 Smit, H. G. J., Poyraz, D., Van Malderen, R., Thompson, A. M., Tarasick, D. W., Stauffer, R. M.,

610 Johnson, B. J., and Kollonige, D. E., 2024. New insights from the Jülich Ozone Sonde  
611 Intercomparison Experiment: calibration functions traceable to one ozone reference instrument.  
612 *Atmospheric Measurement Techniques*, 17, 73–112, <https://doi.org/10.5194/amt-17-73-2024>.

613 Smit, H.G.J., Thompson, A.M., and the ASOPOS 2.0 Panel, 2021. Ozonesonde Measurement  
614 Principles and 1300 Best Operational Practices, WMO Global Atmosphere Watch Report  
615 Series, No. 268, World Meteorological Organization, 1301 Geneva, [Available online at  
616 [https://library.wmo.int/doc\\_num.php?explnum\\_id=10884](https://library.wmo.int/doc_num.php?explnum_id=10884)].

617 Solomon, S., 1999. Stratospheric ozone depletion: A review of concepts and history. *Reviews of*  
618 *Geophysics*, 37(3), 275-316.

619 Staehelin, J., Harris, N.R., Appenzeller, C. and Eberhard, J., 2001. Ozone trends: A review. *Reviews*  
620 *of Geophysics*, 39(2), 231-290.

621 Staufer, J., Staehelin, J., Stübi, R., Peter, T., Tummon, F., Thouret, V., 2013. Trajectory matching of  
622 ozonesondes and MOZAIC measurements in the UTLS - Part 1: Method description and  
623 application at Payerne, Switzerland. *Atmospheric Measurement Techniques*, 6, 3393-3406.  
624 doi:10.5194/amt-6-3393-2013.

625 Staufer, J., Staehelin, J., Stübi, R., Peter, T., Tummon, F., Thouret, V., 2014. Trajectory matching of  
626 ozonesondes and MOZAIC measurements in the UTLS - Part 2: Application to the global  
627 ozonesonde network. *Atmospheric Measurement Techniques*, 7, 241-266. doi:10.5194/amt-7-  
628 241-2014.

629 Stübi, R., Levrat, G., Hoegger, B., Viatte, P., Staehelin, J., Schmidlin, F.J., 2008. In-flight  
630 comparison of Brewer-Mast and electrochemical concentration cell ozonesondes. *Journal of*  
631 *Geophysical Research: Atmospheres*, 113(D13). <https://doi.org/10.1029/2007JD009091>.

632 Tanimoto, H., Zbinden, R.M., Thouret, V., Nédélec, P., 2015. Consistency of tropospheric ozone  
633 observations made by different platforms and techniques in the global databases. *Tellus B:*  
634 *Chemical and Physical Meteorology*, 67(1), 27073.

635 Tarasick, D. W., Davies, J., Anlauf, K., Watt, M., Steinbrecht, W., Claude, H. J., 2002. Laboratory  
636 investigations of the response of Brewer-Mast ozonesondes to tropospheric ozone. *Journal of*  
637 *Geophysical Research: Atmospheres*, 107(D16), ACH-14,  
638 <https://doi.org/10.1029/2001JD001167>.

639 Tarasick, D. W., Davies, J., Smit, H. G., Oltmans, S. J., 2016. A re-evaluated Canadian ozonesonde  
640 record: measurements of the vertical distribution of ozone over Canada from 1966 to 2013.  
641 Atmospheric Measurement Techniques, 9(1), 195-214.

642 Tarasick, D.W., Galbally, I., Cooper, O.R., Schultz, M.G., Ancellet, G., LeBlanc, T., Wallington, T.J.,  
643 Ziemke, J., Liu, X., Steinbacher, M., Stähelin, J., Vigouroux, C., Hannigan, J., García, O., Foret,  
644 G., Zanis, P., Weatherhead, E., Petropavlovskikh, I., Worden, H., Neu, J.L., Osman, M., Liu, J.,  
645 Lin, M., Granados-Muñoz, M., Thompson, A.M., Oltmans, S.J., Cuesta, J., Dufour, G., Thouret,  
646 V., Hassler, B., Thompson, A.M., Trickl, T., 2019. TOAR- Observations: Tropospheric ozone  
647 from 1877 to 2016, observed levels, trends and uncertainties. Elementa: Science of the  
648 Anthropocene, 7(1), 39. DOI: <http://doi.org/10.1525/elementa.376>.

649 Tarasick, D.W., Smit, H.G., Thompson, A.M., Morris, G.A., Witte, J.C., Davies, J., Nakano, T., Van  
650 Malderen, R., Stauffer, R.M., Johnson, B.J., Stübi, R., Oltmans, S.J., Vömel, H., 2021.  
651 Improving ECC ozonesonde data quality: Assessment of current methods and outstanding  
652 issues. Earth and Space Science, 8, e2019EA000914. <https://doi.org/10.1029/2019EA000914>.

653 **Thouret, V., Clark, H., Petzold, A., Nédélec, P., Zahn, A., 2022. IAGOS: Monitoring Atmospheric**  
654 **Composition for Air Quality and Climate by Passenger Aircraft. In Handbook of Air Quality**  
655 **and Climate Change (pp. 1-14). Singapore: Springer Nature Singapore.**

656 Thouret, V., Marenco, A., Logan, J.A., Nédélec, P., Grouhel, C., 1998. Comparisons of ozone  
657 measurements from the MOZAIC airborne program and the ozone sounding network at eight  
658 locations. Journal of Geophysical Research: Atmospheres, 103(D19), 25695-25720. doi:  
659 10.1029/98JD02243.

660 Thompson, A. M., Smit, H. G. J., Witte, J. C., Stauffer, R. M., Johnson, B. J., Morris, G., von der  
661 Gathen, P., Van Malderen, R., Davies, J., Piters, A., Allaart, M., Posny, F., Kivi, R., Cullis, P.,  
662 Hoang Anh, N. T., Corrales, E., Machinini, T., da Silva, F. R., Paiman, G., Thiong'o, K., Zainal,  
663 Z., Brothers, G. B., Wolff, K. R., Nakano, T., Stübi, R., Romanens, G., Coetzee, G. J. R., Diaz,  
664 J. A., Mitro, S., Mohamad, M., Ogino, S., 2019. Ozonesonde quality assurance: The JOSIE-  
665 SHADOZ (2017) experience. Bulletin of the American Meteorological Society, 100(1), 155-  
666 171.

667 Vingarzan, R., 2004. A review of surface ozone background levels and trends. Atmospheric

668 Environment, 38(21), 3431-3442.

669 Vömel, H., Smit, H. G. J., Tarasick, D., Johnson, B., Oltmans, S. J., Selkirk, H., Thompson, A. M.,  
670 Stauffer, R. M., Witte, J. C., Davies, J., van Malderen, R., Morris, G. A., Nakano, T., Stübi, R.,  
671 2020. A new method to correct the electrochemical concentration cell (ECC) ozonesonde time  
672 response and its implications for “background current” and pump efficiency, *Atmospheric  
673 Measurement Techniques*, 13, 5667-5680, <https://doi.org/10.5194/amt-13-5667-2020>.

674 Wang, H., Ke, Y., Tan, Y., Zhu, B., Zhao, T., Yin, Y., 2023. Observational evidence for the dual roles  
675 of BC in the megacity of eastern China: Enhanced O<sub>3</sub> and decreased PM<sub>2.5</sub>  
676 pollution. *Chemosphere*, 327, 138548.

677 Wang, H., Lu, X., Jacob, D.J., Cooper, O.R., Chang, K.L., Li, K., Gao, M., Liu, Y., Sheng, B., Wu, K.,  
678 Wu, T., 2022. Global tropospheric ozone trends, attributions, and radiative impacts in 1995-2017:  
679 an integrated analysis using aircraft (IAGOS) observations, ozonesonde, and multi-decadal  
680 chemical model simulations. *Atmospheric Chemistry and Physics*, 22(20), 13753-13782.

681 Wang, T., Xue, L., Brimblecombe, P., Lam, Y.F., Li, L., Zhang, L., 2017. Ozone pollution in China:  
682 A review of concentrations, meteorological influences, chemical precursors, and  
683 effects. *Science of the Total Environment*, 575, 1582-1596.

684 Williamson, C.E., Neale, P.J., Hylander, S., Rose, K.C., Figueroa, F.L., Robinson, S.A., Häder, D.P.,  
685 Wängberg, S.Å., Worrest, R.C., 2019. The interactive effects of stratospheric ozone depletion,  
686 UV radiation, and climate change on aquatic ecosystems. *Photochemical and Photobiological  
687 Sciences*, 18(3), 717-746.

688 Xu, J., Huang, X., Wang, N., Li, Y., Ding, A., 2021. Understanding ozone pollution in the Yangtze  
689 River Delta of eastern China from the perspective of diurnal cycles. *Science of the Total  
690 Environment*, 752, 141928.

691 Yang, T., Li, H., Wang, H., Sun, Y., Chen, X., Wang, F., Xu, L., Wang, Z., 2023. Vertical aerosol  
692 data assimilation technology and application based on satellite and ground lidar: A review and  
693 outlook. *Journal of Environmental Sciences*, 123, 292-305.

694 Young, P.J., Naik, V., Fiore, A.M., Gaudel, A., Guo, J., Lin, M.Y., Neu, J.L., Parrish, D.D., Rieder,  
695 H.E., Schnell, J.L., Tilmes, S., 2018. Tropospheric Ozone Assessment Report: Assessment of  
696 global-scale model performance for global and regional ozone distributions, variability, and



697 trends. *Elementa: Science of the Anthropocene*, 6.

698 Yu, R., Lin, Y., Zou, J., Dan, Y., Cheng, C., 2021. Review on atmospheric Ozone pollution in China:  
699 Formation, spatiotemporal distribution, precursors and affecting factors. *Atmosphere*, 12(12),  
700 1675.

701 Zang, Z., Liu, J., Tarasick, D., Moeini, O., Bian, J., Zhang, J., Thompson, A. M., Van Malderen, R., Smit,  
702 H. G. J., Stauffer, R. M., Johnson, B. J., Kollonige, D. E., 2024. An improved Trajectory-mapped  
703 Ozonesonde dataset for the Stratosphere and Troposphere (TOST): update, validation and  
704 applications, *EGUsphere* [preprint], <https://doi.org/10.5194/egusphere-2024-800>, 2024.

705 Zbinden, R.M., Thouret, V., Ricaud, P., Carminati, F., Cammas, J.P., Nédélec, P., 2013. Climatology of  
706 pure tropospheric profiles and column contents of ozone and carbon monoxide using MOZAIC in  
707 the mid-northern latitudes (24° N to 50° N) from 1994 to 2009. *Atmospheric Chemistry and Physics*,  
708 13(24), 12363-12388, <https://doi.org/10.5194/acp-13-12363-2013>, 2013.

709 Zhang, L., Jacob, D.J., Boersma, K.F., Jaffe, D.A., Olson, J.R., Bowman, K.W., Worden, J.R., Thompson,  
710 A.M., Avery, M.A., Cohen, R.C., Dibb, J.E., 2008. Transpacific transport of ozone pollution and the  
711 effect of recent Asian emission increases on air quality in North America: an integrated analysis  
712 using satellite, aircraft, ozonesonde, and surface observations. *Atmospheric Chemistry and*  
713 *Physics*, 8(20), 6117-6136.

714 Zhao, K., Huang, J., Wu, Y., Yuan, Z., Wang, Y., Li, Y., Ma, X., Liu, X., Ma, W., Wang, Y., Zhang,  
715 X., 2021. Impact of stratospheric intrusions on ozone enhancement in the lower troposphere  
716 and implication to air quality in Hong Kong and other South China regions. *Journal of*  
717 *Geophysical Research: Atmospheres*, 126(18), e2020JD033955.

## Figures

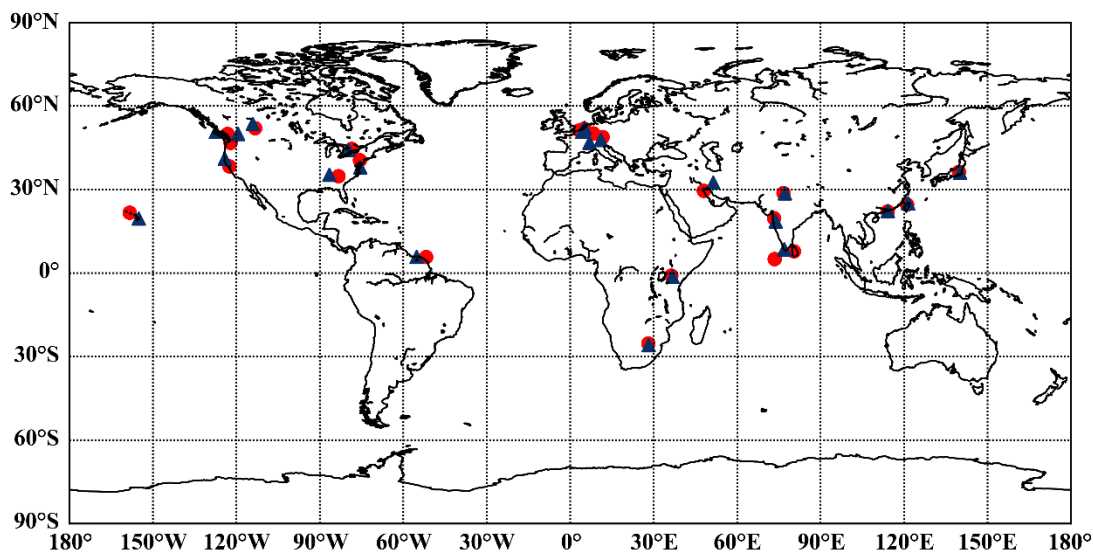


**Figure 1.** Map of 23 pairs of sites used in this study. Red circle markers are IAGOS sites, blue triangle markers are WOUDC sites.

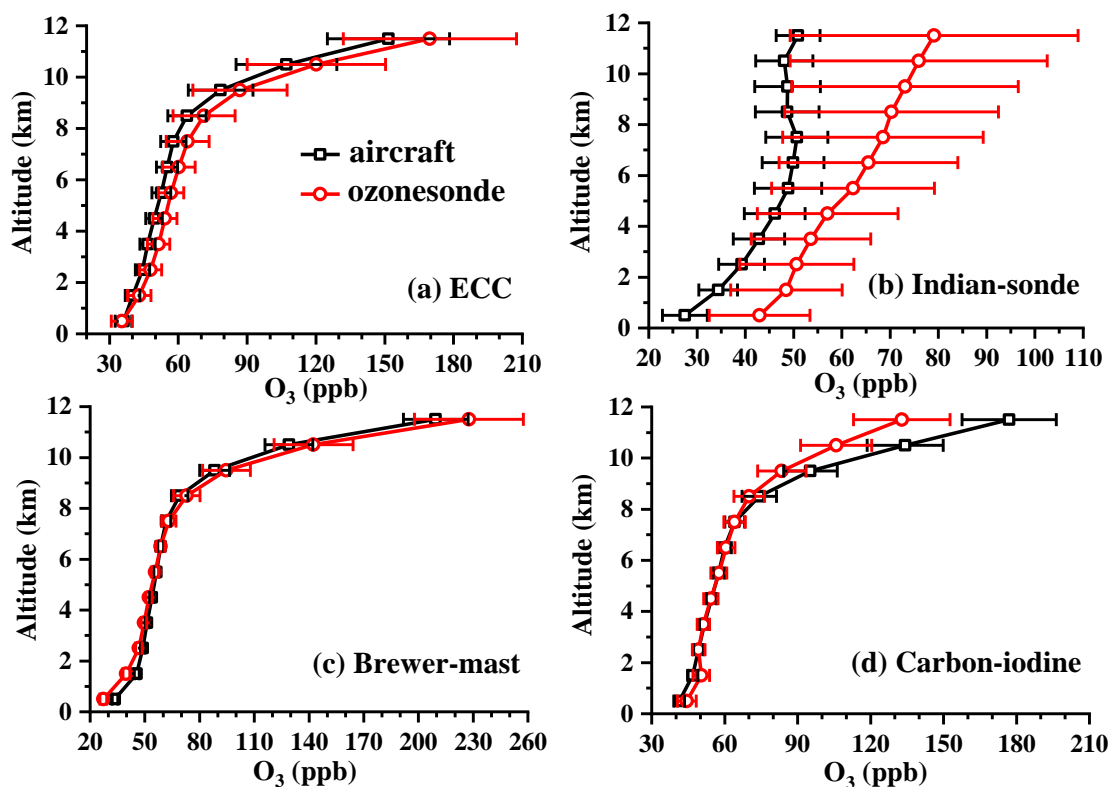


**Figure 2.** Comparison of the vertical profiles of tropospheric  $O_3$  observed between aircraft measurements and four types of ozonesondes, ECC, Indian-sonde, Brewer-mast, and Carbon-iodine. The error bar length is 4 times the standard error (SE) of the mean (equivalent to 95% confidence limits on the averages).

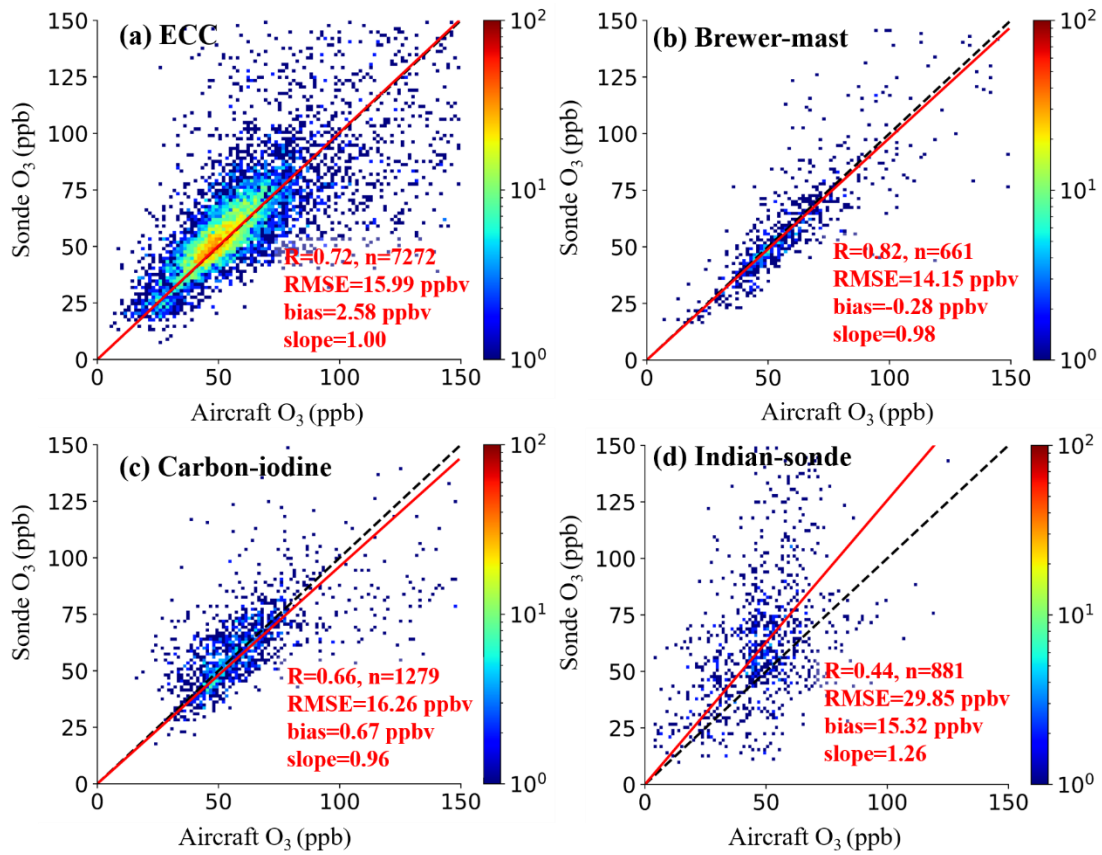


**Figure 3.** Correlation ( $R$ ) of monthly mean ozone mixing ratios between ozonesonde and aircraft measurements. While IAGOS does measure in the lower stratosphere these values are usually far from the airport, so the sonde-aircraft distance will be large, we only plots data below 150 ppb. The black dashed line shows the 1:1 axis, the red line shows the linear fit (with the intercept set to 0), the color bar shows the data counts. Correlations are significant at the 99% level ( $p < 0.01$ ).  $N$  denotes the number of data points,  $R$  is the correlation coefficient, Bias is the overall average difference in monthly mean values [Ozonesonde ozone – Aircraft ozone, in ppb], RMSE is the root mean square error, slope is the slope of the linear fit line. All data points are based on the monthly mean.

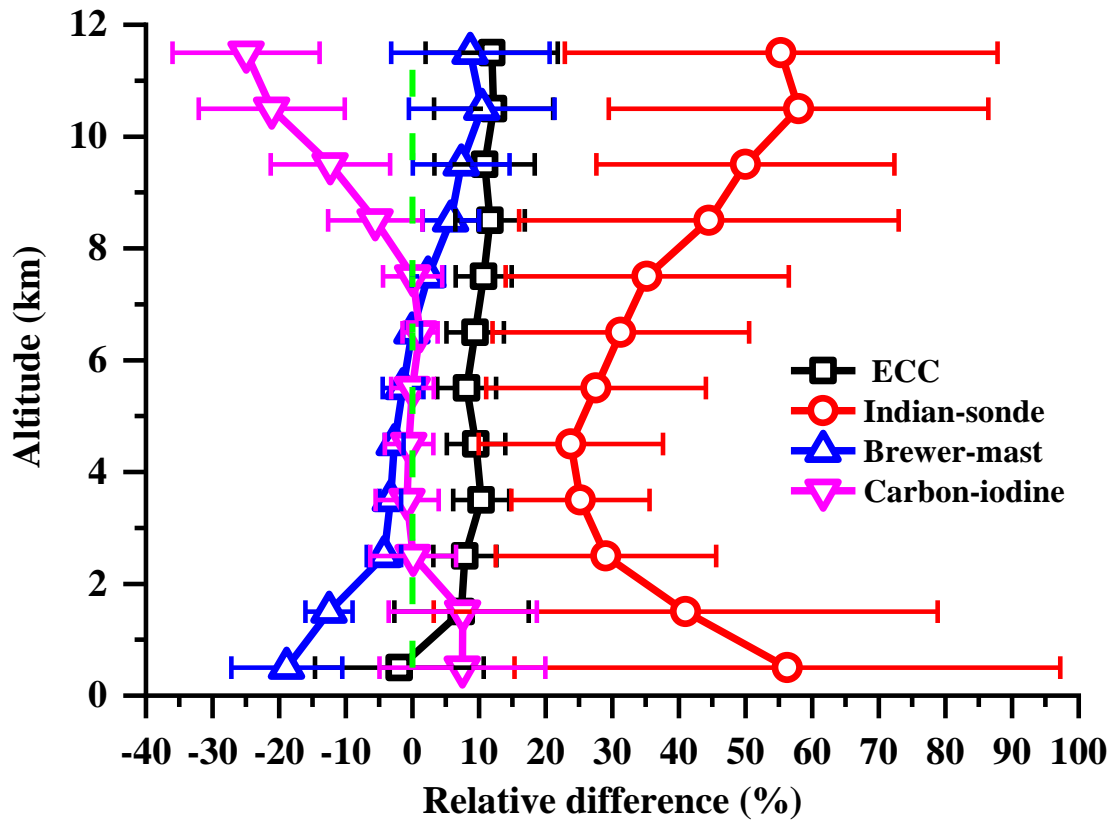


**Figure 4.** Mean relative difference (RD) between the ozonesonde  $O_3$  and aircraft  $O_3$  data. RD is calculated from  $(O_3\text{-ozonesonde} - O_3\text{-aircraft}) / O_3\text{-aircraft} \times 100\%$ . The green dashed line is the zero line.

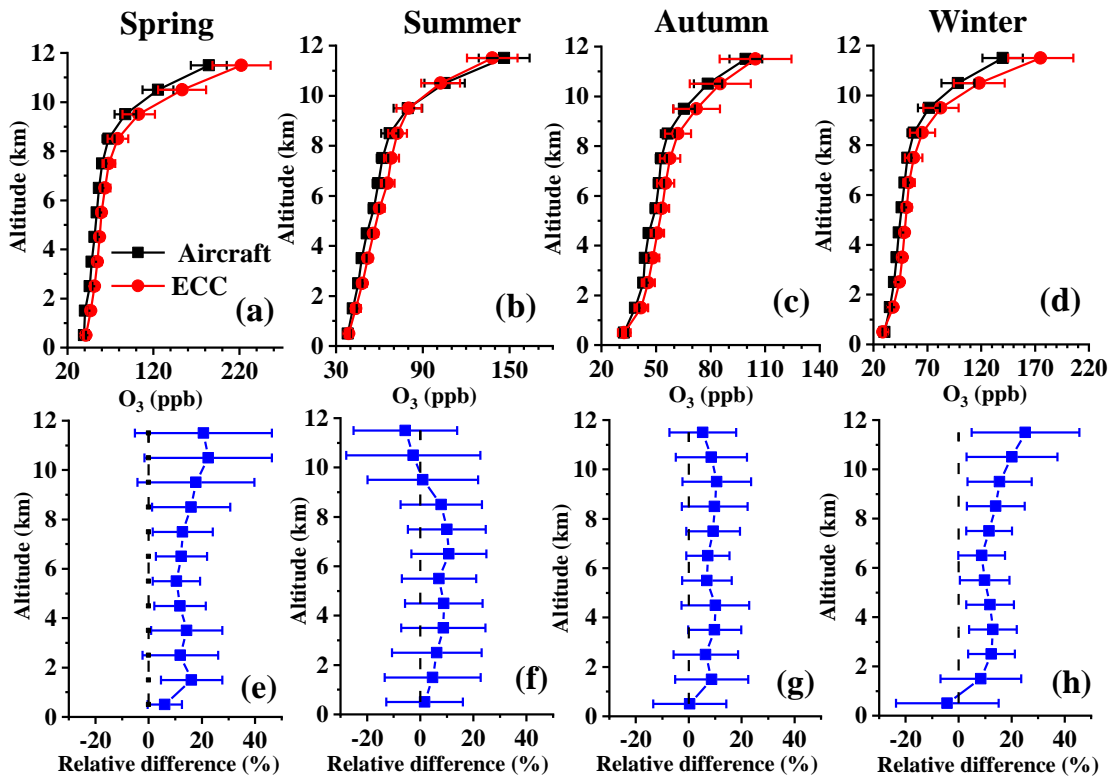


**Figure 5.** The mean difference in vertical profiles of the tropospheric O<sub>3</sub> between ECC ozonesonde and aircraft observations in four seasons (a-d) and their mean relative difference, the black dashed line is the zero line (e-h).

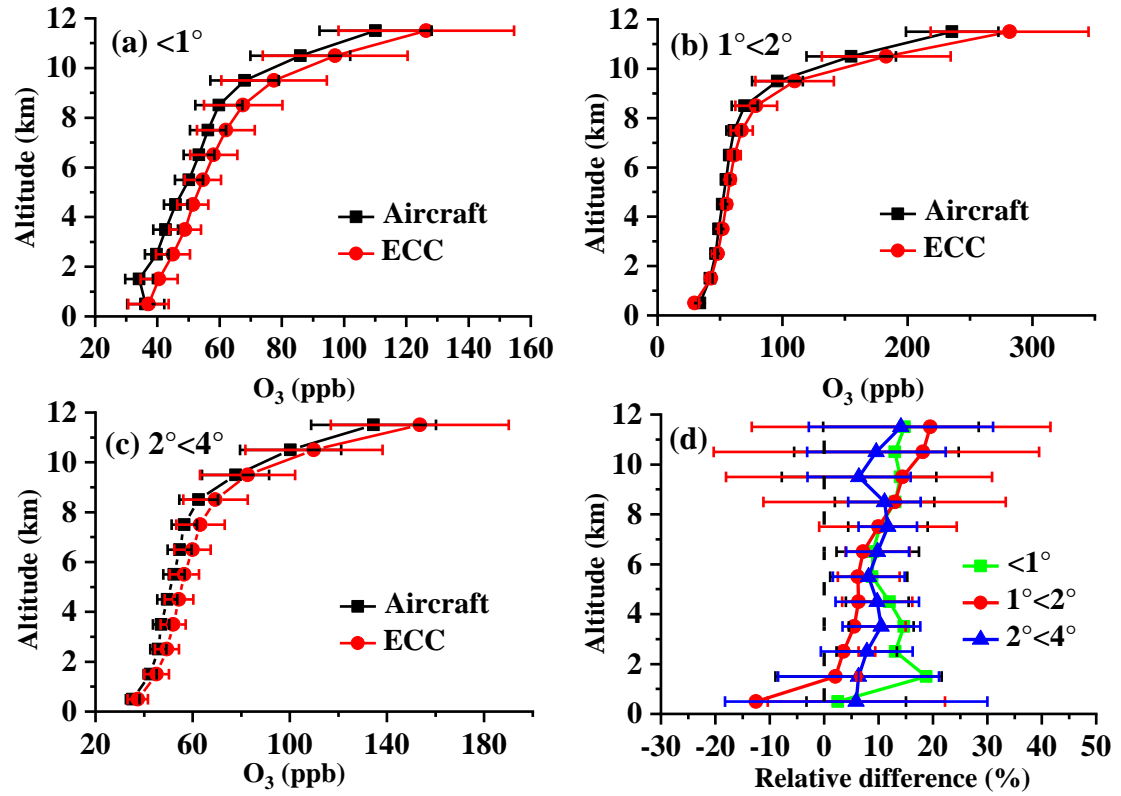


**Figure 6.** The annual mean vertical profiles of tropospheric O<sub>3</sub> between ECC ozonesonde and aircraft observations at station-pair distances (D) of  $D < 1^\circ$  (a),  $1^\circ < D < 2^\circ$  (b), and  $2^\circ < D < 4^\circ$ . The relative differences for the three categories are shown in (d), the black dashed line is the zero line.

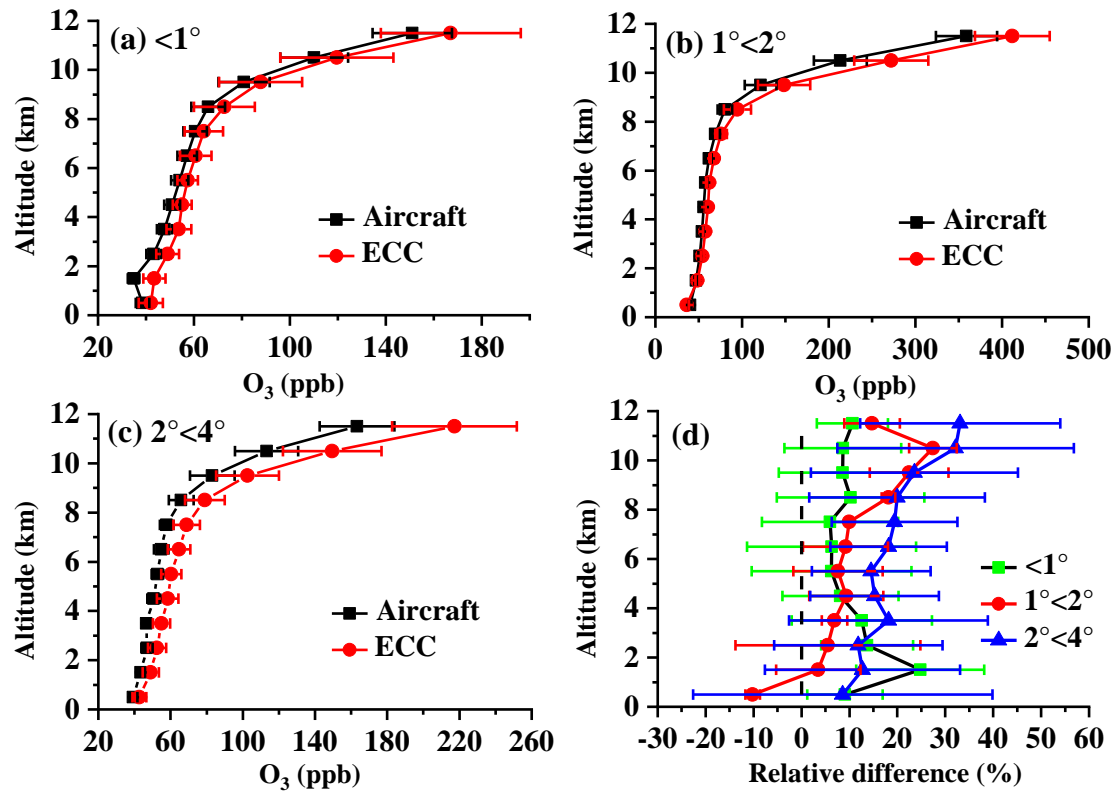


**Figure 7.** The seasonal mean vertical profiles of tropospheric O<sub>3</sub> in spring between ECC ozonesonde and aircraft observations at station-pair distances ( $D$ ) of  $D < 1^\circ$  (a),  $1^\circ < D < 2^\circ$  (b), and  $2^\circ < D < 4^\circ$ . The relative differences for the three categories are shown in (d), the black dashed line is the zero line.

## Tables

**Table 1.** Summary of the station information, including station's name, geolocation, the number of profiles, observational period, and the station-pair distance used in this study.

| MOZAIC-IAGOS |        |        | WOUDC        |                  |        |        | Station- airport |               | No. valid data |        | observation |  |
|--------------|--------|--------|--------------|------------------|--------|--------|------------------|---------------|----------------|--------|-------------|--|
| Station name | Lon    | Lat    | No. profiles | Station name     | Lon    | Lat    | No. profiles     | Type          | distance (km)  | months | period      |  |
| Toronto      | -78.50 | 44.58  | 321          | Egbert           | -79.78 | 44.23  | 181              | ECC           | 108.87         | 33     | 2004-2008   |  |
| Dusseldorf   | 4.96   | 51.82  | 412          | De Bilt          | 5.18   | 52.10  | 333              | ECC           | 34.59          | 63     | 1995-2013   |  |
| Munich       | 11.78  | 48.35  | 2136         | Hohenpeissenberg | 11.02  | 47.81  | 1032             | Brewer-mast   | 82.42          | 67     | 1996-2006   |  |
| Johannesburg | 28.07  | -25.32 | 199          | Irene            | 28.22  | -25.91 | 135              | ECC           | 67.30          | 26     | 1998-2003   |  |
| Nairobi      | 36.33  | -0.94  | 114          | Nairobi          | 36.75  | -1.30  | 42               | ECC           | 61.50          | 10     | 1997-1998   |  |
| Mumbai       | 73.26  | 19.05  | 122          | Pune             | 73.85  | 18.53  | 56               | Indian-sonde  | 84.85          | 35     | 1996-2003   |  |
| Delhi        | 76.65  | 28.73  | 342          | New Delhi        | 77.18  | 28.63  | 88               | Indian-sonde  | 52.88          | 50     | 1995-2016   |  |
| Hongkong     | 114.11 | 22.10  | 123          | King's Park      | 114.17 | 22.31  | 115              | ECC           | 24.15          | 25     | 2000-2005   |  |
| Taipei       | 121.08 | 24.59  | 2115         | Taipei           | 121.48 | 25.02  | 58               | ECC           | 62.58          | 31     | 2014-2018   |  |
| Tokyo        | 139.73 | 36.33  | 1342         | Tateno (Tsukuba) | 140.13 | 36.05  | 655              | Carbon-iodine | 47.52          | 116    | 1995-2006   |  |

|               |         |       |       |                     |         |       |      |              |        |     |           |
|---------------|---------|-------|-------|---------------------|---------|-------|------|--------------|--------|-----|-----------|
| Calgary       | -113.25 | 52.03 | 170   | Edmonton            | -114.10 | 53.55 | 112  | ECC          | 178.41 | 17  | 2009-2011 |
| Brussels      | 3.24    | 51.21 | 2412  | Uccle               | 4.36    | 50.80 | 736  | ECC          | 148.40 | 55  | 1997-2009 |
| Honolulu      | -158.33 | 21.66 | 169   | Hilo (HI)           | -155.07 | 19.58 | 107  | ECC          | 410.56 | 16  | 2015-2017 |
| Vancouver     | -123.14 | 49.95 | 595   | Kelowna             | -127.38 | 50.69 | 594  | ECC          | 312.01 | 68  | 2003-2015 |
| San-Francisco | -122.50 | 38.30 | 34    | Trinidad Head (CA)  | -124.15 | 41.05 | 53   | ECC          | 336.78 | 10  | 1999-2001 |
| Portland      | -122.06 | 46.76 | 385   | Kelowna             | -119.38 | 49.97 | 317  | ECC          | 408.08 | 45  | 2003-2009 |
| Atlanta       | -83.28  | 34.78 | 34    | Huntsville (AL)     | -86.58  | 35.28 | 85   | ECC          | 305.54 | 10  | 1999-2006 |
| Washington    | -75.59  | 40.52 | 610   | Wallops Island (VA) | -75.46  | 37.94 | 616  | ECC          | 287.09 | 80  | 1994-2014 |
| Cayenne       | -51.78  | 5.75  | 200   | Paramaribo          | -55.21  | 5.81  | 64   | ECC          | 379.50 | 9   | 2002-2013 |
| Frankfurt     | 8.30    | 50.16 | 12742 | Payenne             | 6.94    | 46.81 | 2673 | ECC          | 385.72 | 204 | 2002-2020 |
| Kuwait-City   | 48.01   | 29.52 | 105   | Esfahan             | 51.43   | 32.48 | 34   | ECC          | 463.15 | 17  | 2001-2004 |
| Male          | 73.51   | 5.00  | 76    | Trivandrum          | 76.95   | 8.48  | 45   | Indian-sonde | 543.73 | 24  | 1997-2000 |
| Colombo       | 80.41   | 7.79  | 31    | Trivandrum          | 76.95   | 8.48  | 37   | Indian-sonde | 388.49 | 11  | 1998-2000 |



1 **Table 2.** Bias, correlation coefficient (R), and RMSE for four types of ozonesonde and aircraft  
 2 observations in four seasons.

| Type          | Season | Bias ( $O_3$ -ozonesonde - $O_3$ -aircraft) (ppb) | R    | RMSE (ppb) |
|---------------|--------|---|------|------------|
| ECC           | Spring | 17.34   | 0.76 | 65.52      |
|               | Summer | 1.96  | 0.76 | 40.15      |
|               | Autumn | 1.75  | 0.71 | 34.47      |
|               | Winter | 7.61  | 0.71 | 51.74      |
| Brewer-mast   | Spring | 10.22   | 0.94 | 43.51      |
|               | Summer | 2.99  | 0.83 | 48.79      |
|               | Autumn | 6.53  | 0.79 | 29.40      |
|               | Winter | 6.11  | 0.88 | 45.45      |
| Carbon-iodine | Spring | -9.19   | 0.84 | 38.34      |
|               | Summer | 3.83  | 0.46 | 29.31      |
|               | Autumn | 2.33  | 0.68 | 15.10      |
|               | Winter | -16.68  | 0.88 | 44.72      |
| Indian-sonde  | Spring | 19.64   | 0.44 | 44.30      |
|               | Summer | 19.58   | 0.57 | 37.44      |
|               | Autumn | 20.38   | 0.45 | 37.30      |
|               | Winter | 40.07   | 0.18 | 64.99      |

3  
 4 **Table 3.** Bias, correlation coefficient(R) and RMSE for ECC and Indian-sonde ozonesonde and  
 5 aircraft observations at different station-airport distances.

| Type         | Station-pair distance | Bias ( $O_3$ -ozonesonde - $O_3$ -aircraft) (ppb) | R    | RMSE (ppb) |
|--------------|-----------------------|---|------|------------|
| ECC          | <1°                   | 9.78  | 0.78 | 47.46      |
|              | 1°-2°                 | 8.91  | 0.90 | 40.73      |
|              | 2°-4°                 | 5.65  | 0.67 | 51.00      |
| Indian-sonde | <1°                   | 26.71   | 0.37 | 49.54      |
|              | 2°-4°                 | 15.35   | 0.24 | 30.86      |

6

7 **Table 4.** Comparison of the sondes of each type to IAGOS. (average  $\pm$  2 times the standard error  
 8 (SE)) Indian-sonde/ECC is (Indian-sonde/IAGOS)/(ECC/IAGOS), Brewer-mast/ECC is (Brewer-  
 9 mast/IAGOS)/(ECC/IAGOS), Carbon-iodine/ECC is (Carbon-iodine /IAGOS)/(ECC/IAGOS)

| Altitude(km) | Indian-sonde/ECC | Brewer-mast/ECC | Carbon-iodine/ECC | ECC/ IAGOS      |
|--------------|------------------|-----------------|-------------------|-----------------|
| 0-1          | 1.59 $\pm$ 1.74  | 0.83 $\pm$ 0.96 | 1.10 $\pm$ 1.36   | 0.98 $\pm$ 1.28 |
| 1-2          | 1.31 $\pm$ 1.83  | 0.81 $\pm$ 0.90 | 1.00 $\pm$ 1.05   | 1.07 $\pm$ 1.58 |
| 2-3          | 1.20 $\pm$ 1.62  | 0.89 $\pm$ 0.97 | 0.93 $\pm$ 0.85   | 1.08 $\pm$ 1.54 |
| 3-4          | 1.14 $\pm$ 1.57  | 0.88 $\pm$ 0.94 | 0.90 $\pm$ 0.87   | 1.10 $\pm$ 1.48 |
| 4-5          | 1.13 $\pm$ 1.61  | 0.89 $\pm$ 1.02 | 0.91 $\pm$ 0.99   | 1.10 $\pm$ 1.44 |
| 5-6          | 1.18 $\pm$ 1.76  | 0.91 $\pm$ 1.05 | 0.92 $\pm$ 1.04   | 1.08 $\pm$ 1.37 |
| 6-7          | 1.20 $\pm$ 1.89  | 0.91 $\pm$ 1.00 | 0.92 $\pm$ 0.82   | 1.09 $\pm$ 1.54 |
| 7-8          | 1.22 $\pm$ 1.92  | 0.92 $\pm$ 0.94 | 0.90 $\pm$ 0.64   | 1.11 $\pm$ 1.69 |
| 8-9          | 1.29 $\pm$ 2.09  | 0.95 $\pm$ 0.99 | 0.85 $\pm$ 0.55   | 1.12 $\pm$ 1.61 |
| 9-10         | 1.35 $\pm$ 2.35  | 0.97 $\pm$ 1.09 | 0.79 $\pm$ 0.62   | 1.11 $\pm$ 1.46 |
| 10-11        | 1.41 $\pm$ 3.26  | 0.98 $\pm$ 1.21 | 0.70 $\pm$ 0.68   | 1.12 $\pm$ 1.37 |
| 11-12        | 1.39 $\pm$ 4.61  | 0.97 $\pm$ 1.19 | 0.67 $\pm$ 0.72   | 1.12 $\pm$ 1.42 |

10